Journal of the European Ceramic Society **19** (1999) 247–253

PII: S0955-2219(98)00195-2
0955-2219/98/$—see front matter

Strengthening Contribution Arising from Residual Stresses in Al_2O_3/ZrO_2 Composites: a Piezo-Spectroscopy Investigation

Giuseppe Pezzotti,[a]* Valter Sergo,[b] Orfeo Sbaizero,[b] Naoki Muraki,[c] Sergio Meriani[b] and Toshihiko Nishida[b]

[a]Department of Materials, Kyoto Institute of Technology, Sakyo-ku, Matsugasaki, Kyoto-shi 606, Japan
[b]Materials Engineering and Applied Chemistry Department, University of Trieste, Via Valerio 2, 34127 Trieste, Italy
[c]Toray Research Center, Inc., 3-3-7, Sonoyama, Otsu-shi, Shiga 520, Japan

(Received 28 March 1998; accepted 30 July 1998)

Abstract

Piezo-spectroscopy measurements have been performed in order to obtain information about the internal stresses in a series of (2 mol% Y_2O_3-stabilized) ZrO_2 ceramics added with fine Al_2O_3 dispersoids. These composites were previously reported to fracture at remarkably high strength levels. Residual stresses arising from the thermal mismatch between the ZrO_2 matrix and the Al_2O_3 dispersoids were found to be of the order of several hundreds MPa, in agreement with the predictions of an elastic stochastic stress analysis. Taking into consideration the results of the present piezo-spectroscopic analysis, a micromechanism of microcrack shielding by residual microstresses has been proposed, which overlaps with the effect of phase transformation on strength. A theoretical assessment is given which enables one to explain the presence of a maximum of strength at 0·2–0·4 volume fraction of Al_2O_3 dispersoid. © *1998 Elsevier Science Limited. All rights reserved*

Keywords: ZrO_2, Al_2O_3, composites, residual stresses, strength.

1 Introduction

Two micromechanical arguments have been proposed for explaining the superior strength behavior found in ZrO_2-based alloys and composite materials:[1–5] (i) the contribution of internal stresses arising from the transformation of ZrO_2 from tetragonal to monoclinic phase (*t*- to *m*-ZrO_2 transformation) in a process zone around the crack tip and, (ii) the inherent rising *R*-curve behavior by bridging effects along the crack wake. As a consequence of the aforementioned two circumstances, analyses by linear elastic fracture mechanics usually fail to explain the mechanical performance of transformation-toughened ZrO_2 ceramics. In other words, a marked non-proportionality between strength and toughness is found. The mechanical behavior of several ZrO_2-based alloys has been recently discussed by Swain and Rose.[6] These researchers provided both experimental evidence and theoretical foundation to support either phase transformation-related residual stress or *R*-curve strengthening contributions, depending on the magnitude of the inherent crack extension.

Besides the well established mechanical response of those alloyed ZrO_2 materials, however, the behavior of ZrO_2-based composites remains yet to be explained. For example, Shikata *et al.*[7–9] reported some extremely high strength value (i.e. $\approx$3 GPa) for a ZrO_2 matrix added with few tens percent Al_2O_3 particles. In the fracture of those materials (fairly brittle relatively to the ZrO_2 alloys described by Swain and Rose[6]), relevant contribution to strength by a rising *R*-curve behavior is not expected. The rationale for this assertion may reside in the very fine (submicrometer) size of both matrix grains and dispersoids. With increasing Al_2O_3 fraction, which is not transforming, one would expect a monotonic decrease in strength rather than a strengthening effect. This prediction is not confirmed by experiments which show instead a maximum in strength at relatively low fractions of Al_2O_3. In addition, the maximum of strength experienced by these composites was about twice the level found in monolithic ZrO_2,

*To whom correspondence should be addressed.

thus implying that only arguments based on shielding effects due to ZrO_2 phase-transformation are not suitable to fully explain the strength behavior of these materials.

We propose here that a further micromechanical circumstance may provide a strengthening effect: the presence of remarkable (microscopic) residual stresses arising from the thermal expansion mismatch between ZrO_2 and Al_2O_3 crystallites. In this paper, residual stresses in the Al_2O_3/ZrO_2 composites have been accurately measured by piezo-spectroscopy and a strengthening mechanism based on the presence of such internal stresses proposed and theoretically discussed.

2 Experimental Procedure

The Al_2O_3/ZrO_2 material investigated in this paper was prepared by Shikata *et al.*[7–9] For readers' convenience, the salient processing conditions of this material are given hereafter. Very fine ZrO_2 powder (average size: 0·21 μm) containing 2 mol% Y_2O_3 was added with increasing fractions of submicrometer Al_2O_3 powder (average size: 0·54 μm). After a preforming cycle by cold isostatic pressing a pre-sintering cycle was performed in air at 1500°C for 3 h. The dense composite bodies obtained by the above processing were then hot-isostatically pressed (HIPed) under Ar atmosphere for 1 h at 1450°C under $\approx$100 MPa. A microstructural analysis by scanning electron microscopy (SEM) showed that both the ZrO_2 and Al_2O_3 crystallites composing the final composite bodies were preserving their submicrometer size after processing (Fig. 1).

The spectroscope apparatus used for measuring residual stresses as detected from fluorescence (in Al_2O_3) and from Raman (in ZrO_2) spectra was an ISA, T64000 Jovin-Yvon employing an Ar laser operating at a wavelength of 488 nm with a power of 300 mW and 30 mW for ZrO_2 and Al_2O_3, respectively, as the excitation source. The scattered light was analyzed with a triple monochromator equipped with a charge-coupled device (CCD) camera. The dimension of the laser spot on the samples was fixed at $\approx$10 μm so as to probe many grains simultaneously. The ruby fluorescence[10] was applied for analyzing stresses in the Al_2O_3 phase. The frequency shift due to the applied stress was monitored on the characteristic R_1, R_2 doublet, namely the two ruby fluorescence peaks located at 14 400 and 14 430 cm^{-1}, respectively. The neon line at 14564 cm^{-1} from a neon discharge lamp was used as an external frequency calibration. The peak shift due to temperature fluctuations was corrected using the temperature dependence coefficient of $\approx$0·14 cm^{-1} °C.[11] The shift of the Raman line located at 634 cm^{-1} was monitored in the *t*-ZrO_2 phase. The collected data were analyzed with the curve-fitting algorithms included in the SpectraCalc software package (Galactic Industries Corp.). The average residual stress in the Al_2O_3 and ZrO_2 phase were calculated from the measured frequency shifts according to a relation of linear proportionality through the average piezo-spectroscopic coefficients given in literature.[11,12]

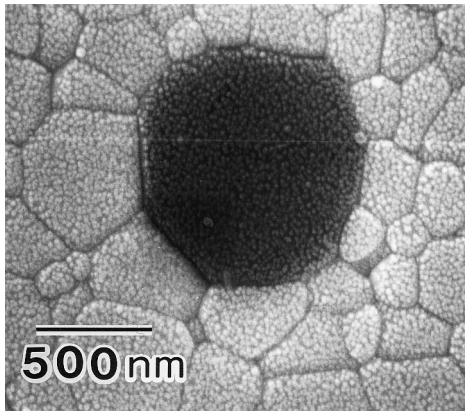

Fig. 1. An Al_2O_3 particle (dark grain) surrounded by submicrometer-sized ZrO_2 grains as observed by SEM.

3 Results

3.1 Mechanical behavior

Strength and toughness data for the ZrO_2-based materials as a function of the Al_2O_3 dispersed fraction are plotted in Fig. 2 from Shikata *et al.*[9] A number of interesting characteristic features can be noticed in these data: first, the presence of a strength maximum in the range 20–40 vol% Al_2O_3, which cannot be easily explained just in terms of

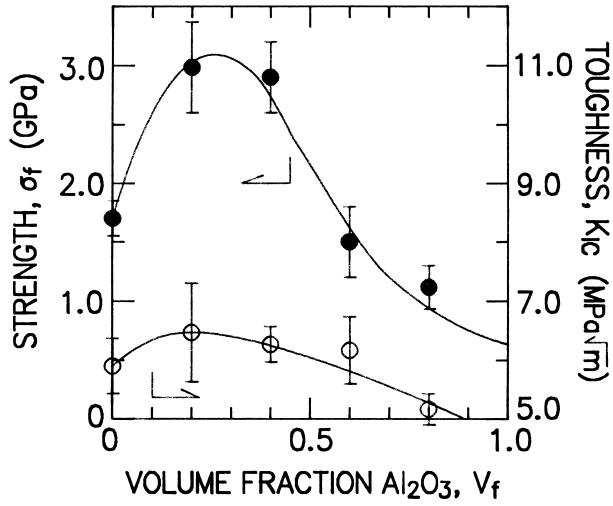

Fig. 2. Fracture strength and toughness data for the Y_2O_3-stabilized ZrO_2 material as a function of the added Al_2O_3 volume fraction.[7–9]

the measured toughness values (i.e. via Griffith's proportionality equation), since the fracture toughness experiences a value scarcely affected by the increasing Al_2O_3 content. The maximum of strength experiences the rather high value of ≈ 3 GPa although it drops down to less than half for Al_2O_3 contents > 40 wt%. In addition, owing to the fact that the above fracture toughness data were obtained by a test method employing a long pre-crack subjected to shielding forces (i.e., by the single-edge pre-cracked beam method[13]), it can be argued that any *R*-curve contribution should be already included in the K_{IC} values of Fig. 2. Furthermore, the addition of an increasing fraction of non-transforming Al_2O_3 dispersoids should conceivably lead to a monotonic decrease in strength, whereas in Fig. 2 such a decrease is observed only at rather large Al_2O_3 fractions. A theoretical model aimed to rationalize all these experimental features is proposed in Section 4.

3.2 Residual stresses

The results of piezo-spectroscopic experiments carried out to determine the residual stresses are shown in Fig. 3. As seen, in the range of volume fractions of Al_2O_3 dispersoids, V_f, pertinent to the present investigation (i.e. up to ≈ 40 vol%), data can be fitted very accurately to a linear dependence. Ma *et al.*[11] reported that, in composites with the same nominal composition as those examined here but with cubic ZrO_2, stress relaxation may occur for $V_f < 20\%$; in fact, the dependence of the residual stress on V_f deviates from a linear behavior. Such a relaxation effect could not be noticed in the present experiments. This may be due to the different grain size of both matrix and dispersoids

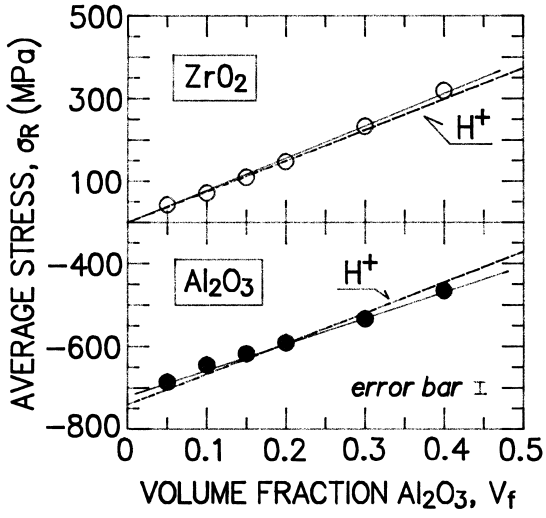

Fig. 3. Experimental data of residual stresses, as determined by piezo-spectroscopy measurements in the ZrO_2 and Al_2O^3 phases, are compared with the theoretical predictions of elastic stochastic stress analysis.[14] The broken lines represent the upper Hashin bound (H^+) for the elastic stresses.

which, in the composites studied by Ma *et al.* was about one order of magnitude larger than that of the present materials. An attempt to estimate the reliability of the present residual stress data is presented hereafter based on the stochastic microstress analysis by Kreher and Pompe.[14]

The average isotropic part of residual stress in the matrix material, $\langle \sigma^i_{ik} \rangle_m$ can be expressed as

$$\langle \sigma^i_{ik} \rangle_m = s_m \delta_{ik} \tag{1}$$

$$s_m = -\left[3K_m K_d / V_{fm}(K_m - K_d)\right]\{V_{fd} - \left[K_d(K_m - K^*)/K^*(K_m - K_d)\right]\}(\alpha_d - \alpha_m)\Delta T \tag{2}$$

where V_f, K and α are the volume fraction, the bulk modulus and the average coefficient of thermal expansion, respectively; the subscripts m and d refer to the matrix and the dispersed values, respectively (namely the ZrO_2 and Al_2O_3 phase, respectively). δ_{ik} is the Kronecker symbol. Equations (1) and (2) allow to theoretically calculate the stress values to be compared with the experiments, although the elastic stress-free temperature (on cooling), ΔT, is a parameter rather difficult to determine exactly. In the present computation ΔT was assumed to be 1180°C as estimated by Sergo *et al.*[15] The coefficients of thermal expansion of the hexagonal Al_2O_3 phase was calculated as $\alpha_m = (2\alpha_a + \alpha_c)/3$, the subscripts a and c indicating the single-crystal values measured along different crystallographic directions. The value of thermal expansion mismatch in the present composites, comprehensive of the temperature dependence, was assumed as $\langle \Delta\alpha \rangle = (\alpha_d - \alpha_m) = (4{\cdot}6 - 0{\cdot}00124T) \times 10^{-6}\ K^{-1}$ The effective bulk modulus, K^*, is a function of the elastic constants of the constituent phases, their respective volume fractions and topological arrangement. Provided that the microstructures of the present composite materials are statistically isotropic, it can be shown[14] that the effective bulk modulus approaches the upper Hashin limit, K^+, given by the equation:

$$K^* = K^+ = V_{fm}K_m + V_{fd}K_d - \left[V_{fm}V_{fd}(K_m - K_d)^2 / (V_{fm}K_d + V_{fd}K_m + 4G_m/3)\right] \tag{3}$$

where G_m is the shear modulus of the matrix. The elastic constant values pertaining to the present composites are: $K_m = 197$ GPa, $K_d = 130$ GPa and $G_m = 85$ GPa.

The theoretical values for the average isotropic residual stress component in the constituent phases were calculated according to eqns (1) to (3) and

plotted by broken lines in Fig. 3. The theoretical prediction relative to an upper Hashin limit (H^+) satisfactorily fits the experimental stress data. This confirms that, at least for composites with low fractions of Al_2O_3, residual microstresses can be rationalized simply invoking arguments of theory of elasticity.

A further confirmation about the reliability of the present residual stress data can be obtained from force balance considerations. When equilibrium is achieved, the average residual stresses stored in the matrix and the dispersed phases must obey the following relation:

$$V_{fm}\langle\sigma^i_{ik}\rangle_m + V_{fd}\langle\sigma^i_{ik}\rangle_d = 0 \tag{4}$$

It can be shown that this relationship is indeed satisfied by the present spectroscopy data (Fig. 3). This is an encouraging result since the stresses are obtained from two independent phenomena, the shift of luminescence lines (of Cr in Al_2O_3) and that of Raman lines (of ZrO_2). The maximum deviation from the zero value, as calculated from eqn (4), was ± 20 MPa, which is considered to represent the accuracy of the present spectroscopy measurements (cf. error bar in Fig. 3). A more detailed discussion of residual stress data, comprehensive of their dependence on the grain-size of both matrix and dispersoids is given in a separate paper.[16] Hereafter, emphasis is placed on a theoretical treatment aimed to assess the effect of *t*- to *m*-ZrO_2 transformation as well as that of the elastic residual stresses arising from thermal expansion mismatch on the strength behavior of the present composites. The effect of residual stress will be based on elasticity arguments since they have been proved to satisfactorily explain the stress status of the material on the microstructural scale.

4 Discussion

4.1 Contribution to strength of phase transformation

In an ideal brittle material, a plot of strength versus toughness should experience the linear relationship:[17]

$$\sigma_f = K_{IC}/Ya_0^{1/2} \tag{5}$$

where Y is a geometric factor (typically $=1{\cdot}2$ for a semielliptical flaw) while a_0 represents the size of the critical microcrack. Observation of σ_f and K_{IC} plots versus the volume fraction of Al_2O_3 (Fig. 2) immediately envisages that eqn (5) does not apply to the present composites. In other words, the increment of K_{IC}, if any, with increasing V_f, is not sufficient to justify the remarkable maximum of strength found between 20 and 40 vol% Al_2O_3. This apparently contradictory aspect of the mechanical behavior of ZrO_2 materials is well known,[4–6] although no emphasis has been so far placed on the effect of adding a conspicuous fraction of non-transforming particles to a transforming ZrO_2 matrix.

Swain and Rose[6] have analyzed the mechanisms governing the strength level of several transformation-toughened ZrO_2 ceramics. They proposed that, in yttria-tetragonal ZrO_2 polycrystals, the strength is limited by a critical stress which triggers the transformation. Assuming a cardioid-shape transformation zone around the crack, the following expressions for the steady-state toughness and the critical hydrostatic stress exerted on the crack tip can be obtained:[18,19]

$$K_{IC} = K_0 + \beta\sigma^T h^{1/2} \tag{6}$$

$$\sigma_c = \beta(1+\nu_m)K_0/3h^{1/2} \tag{7}$$

where h is the size of the transformation zone, K_0 is the toughness of a ZrO_2 matrix containing pre-transformed precipitates, σ^T is the magnitude of the compressive stresses generated by the transformation, and $\nu_m = 0{\cdot}31$ is the Poisson's ratio of the ZrO_2 polycrystal. The proportionality constant β depends on the precise zone shape and the volume fraction of the non-transforming Al_2O_3 particles:

$$\beta = 0{\cdot}66\left(1 - V_f\right) \tag{8}$$

where the numerical coefficient in eqn (8) as well as a value $\sigma^T = 4{\cdot}36$ GPa have been experimentally determined for yttria-tetragonal ZrO_2 polycrystals.[4,6]

The critical fracture stress is then given by:

$$\sigma_f = 3\sigma_c/(1+\nu) = \beta K_0/h^{1/2} \tag{9}$$

Eliminating $h^{1/2}$ between eqns (6) and (9) and substituting from eqn (8), σ_f becomes:

$$\sigma_f = \left[0{\cdot}66\left(1 - V_f\right)\right]^2\sigma^T[K_0/(K_{IC} - K_0)] \tag{10}$$

A plot of this expression with $K_0 = 3$ MPa $m^{1/2}$ [6] and K_{IC} equal to an average value ≈ 6 MPa $m^{1/2}$ (cf. Fig. 2) is given in Fig. 5 The data plot from eqn (10) for monolithic ZrO_2 (i.e. at $V_f = 0$) is in good agreement with the experimental strength value, confirming the validity of the Swain and Rose model[6] for monolithic ZrO_2. However, according to this model, a non-linear decrease in strength should be found with increasing the fraction of

non-transforming Al_2O_3 particles, a trend which is not supported by experiments. This means that the model of Swain and Rose[6] in its present form cannot explain the actual strength behavior of Al_2O_3/ZrO_2 composites. An additional strengthening mechanism arising from local residual stresses must be considered and it will be proposed in the next section. The σ_f values calculated from eqn (10) should be regarded as the strength of the composite when no strengthening mechanism other than *t*- to *m*-ZrO_2 transformation is operative.

4.2 Contribution to strength of elastic residual stresses

Models of toughening by local cracking or residual stresses have been previously proposed in the literature.[20,21] However, the usefulness of these models in explaining the present data is limited because they mainly deal with toughness rather than with strength. In the present composite, no noticeable toughening effect is found. Here, we deal with a composite material whose strengthening is not arising from a toughening effect. Thus, at first glance, this material does not obey the general criterion of brittle fracture.[22] In order to explain the existence of a maximum in strength (without consistent toughening) at moderate volume fractions of Al_2O_3, we need to figure out a different strengthening mechanism. In this study, we propose that local residual microstresses, arising from the mismatch in thermal expansion between the constitutive phases of the composite, can either shield the microcracks (which trigger catastrophic fracture above the critical stress for phase transformation) or, at least, delay their formation. This micromechanism is schematically depicted in Fig. 4 for the case of a newly formed microcrack.* The Al_3O_3 particles are in a strong compressive stress field which, for the equilibrium, will produce locally high tension in the ZrO_2 matrix. When two dispersoids are sufficiently close and placed on the opposite sides of the microcrack, a shielding (closure) stress component, σ_R, can be generated on

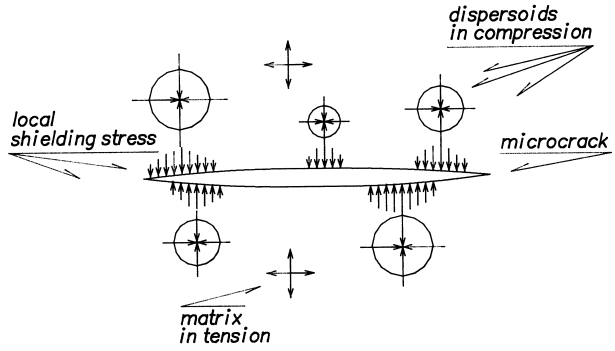

Fig. 4. Schematic representing a possible strengthening effect arising from shielding of a newly formed microcrack by local (compressive) residual stresses.

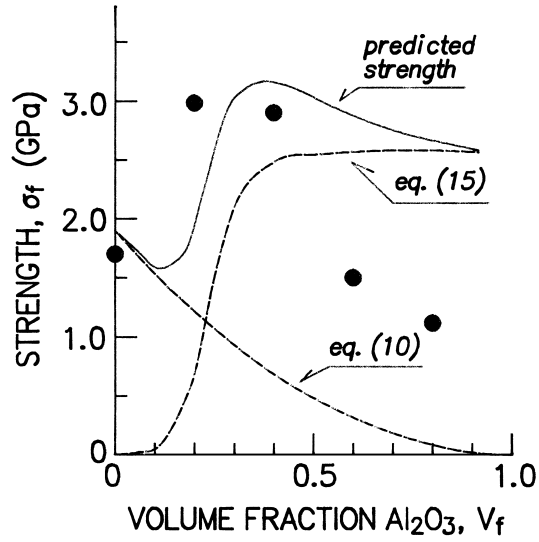

Fig. 5. Experimental data of fracture strength compared with the theoretical predictions based on: (a) transformation toughening model [eqn (10)] and (b) residual stress model [eqn (15)]. The sum of these contributions is also plotted as predicted strength.

the microcrack. The increase in critical stress intensity factor at the tip of the microcrack is given as:[22]

$$\Delta K = 2\sigma_R \Phi (a_0/\pi)^{1/2} \qquad (11)$$

where a_0 is the size of the formed microcrack and Φ a constant depending upon the shape of the microcrack.[23] This geometrical constant can be assumed as $\Phi \approx 2$ for a microcrack subjected to shielding forces over its entire extension. The shielding stress σ_R will be a function of the average (statistical) distance between a microcrack and the Al_2O_3 dispersed. According to elasticity arguments, the stress field around an inclusion showing thermal mismatch with the surrounding matrix decreases with the third power of the distance from the inclusion/matrix interface.[24] Thus, σ_R can be represented with the following expression:

$$\sigma_R = (\sigma_{max}/2)[2d/(\Delta - d)]^3 \qquad (12)$$

*The model depicted in Fig. 4 can represent a general case of local crack-closure mechanism by residual stresses, although, in principle, two statistical exceptions to this model should be recognized: (i) an isolated Al_2O_3 particle is placed just ahead of the microcrack tip; and, (ii) the microcrack is generated at a phase boundary between the Al_2O_3 particle and the ZrO_2 matrix. In both the above cases, the microcrack tip would become subjected to a local tensile stress field. Now, the latter case will hardly occur because the higher thermal expansion coefficient of the Al_2O_3 inclusion, as compared to the ZrO_2 matrix, should hamper the formation of a phase-boundary microcrack during cooling down from sintering temperature. On the other hand, the situation of an isolated inclusion just ahead of the crack tip cannot be statistically ruled out. The low strength arising in this particular case should affect the scatter of the composite strength data.

where Δ is the average near-neighbors distance,[25] d is the grain size of the dispersoid, and the maximum stress magnitude, σ_{max}, arising from the thermal expansion mismatch, $\langle\Delta\alpha\rangle$, is given by:

$$\sigma_{max} = \langle\Delta\alpha\rangle\Delta T/\{[(1+\nu_m)/2E_m] + [(1-2\nu_d)/E_d]\} \quad (13)$$

where E_m (= 205 GPa) and E_d (= 350 GPa) are the Young's moduli of the matrix and the dispersoid, respectively. Assuming the Poisson's ratio of the dispersoid as $\nu_d = 0{\cdot}25$ and the remaining parameters as given in Section 3, σ_{max} can be calculated as $\approx 0{\cdot}45$ GPa. It should be noted that the magnitude of shielding stress, σ_R, depends on the volume fraction of dispersoid, V_f, through the dependence of the near-neighbors distance Δ on V_f [cf. eqn (12)]. The function $\Delta(V_f)$, experimentally determined in previous studies on particle-reinforced composites,[26,27] is plotted in Fig. 6.

Now we can work out an expression for the strength increase, $\Delta\sigma$, due to microcrack shielding by residual stresses, by invoking a Dugdale-like model,[28] namely, under the assumption of a constant shielding force acting on the entire microcrack length. This assumption may be appropriate according to the conceivably small size of the microcrack which triggers catastrophic fracture. This strength increase is given by:

$$\Delta\sigma = \Delta K/Ya_0^{1/2} \quad (14)$$

Substituting from eqns (11)–(13), one obtains the final expression for the strengthening effect by residual stresses:

$$\Delta\sigma = \{\langle\Delta\alpha\rangle\Delta T/\{[(1+\nu_m)/2E_m] + [(1-2\nu_d)/E_d]\}\}[2d/(\Delta - d)]^3\Phi/Y\pi^{1/2} \quad (15)$$

This expression can be used to calculate $\Delta\sigma$ as a function of the volume fraction of dispersoids V_f through the dependence $\Delta = \Delta(V_f)$ given in Fig. 6. The result of this calculation is displayed in Fig. 5 As seen, a curve of sigmoidal shape is obtained, reflecting the strongly non-linear dependence of the stereological parameter Δ on V_f, To allow for a direct comparison with the experimental strength data, the function $\sigma_f + \Delta\sigma$, comprehensive of the phase-transformation [eqn (10)] and the residual stress [eqn (15)] contributions, is also plotted in Fig. 5 together with the experimental data. The sum of the two strength contributions reproduces the maximum of strength which was experimentally observed in the interval $V_f = 0{\cdot}2-0{\cdot}4$. Furthermore, the predicted magnitude of maximum strength agrees tolerably well with the measured value, while an overestimation of strength is found at higher volume fractions of dispersoid. In order to discuss this discrepancy, we notice that both eqns (10) and (15) predict a strength which is independent of the initial flaw size a_0. This is because the postulated micromechanism which triggers catastrophic failure is the presence of a critical stress to induce t to m-ZrO_2 transformation rather than the propagation of a single (critical) pre-existing flaw as stated by the Griffith's criterion for fracture. This hypothesis may indeed break down in presence of high fractions of Al_2O_3 phase, for which a non negligible agglomeration of Al_2O_3 grains occurs. In fact, when large islands of such non-transforming phase are present, pre-existing flaws (i.e. pores or grain boundaries belonging to these islands) may lead to fracture in agreement with the Griffith's criterion.

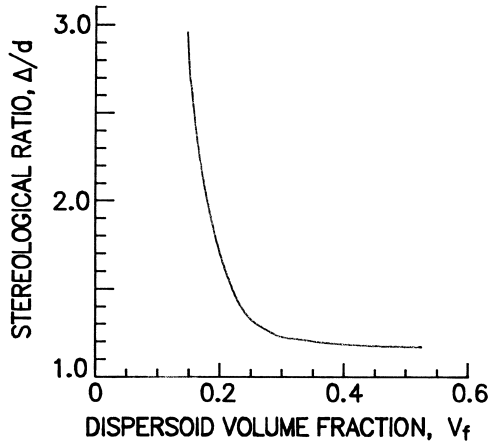

Fig. 6. Stereological dependence of the near-neighbors distance, Δ, on the volume fraction, V_f, of dispersoid.[26,27]

5 Conclusion

Piezo-spectroscopy measurements have been carried out on a series of yttria-tetragonal ZrO_2 polycrystals added with increasing amount of fine Al_2O_3 dispersoids. Due to the thermal expansion mismatch between the constituent phases, microscopic residual stresses were found to remain stored in the composite. The residual stresses experimentally measured compared favourably with the predictions of an elastic stochastic stress analysis. This indicates both that elastic stress arguments can fully explain the residual stress behavior of the present composites and that the piezo-spectroscopy approach provides reliable data. Subsequently, the mechanical behavior of the composites was theoretically analyzed.

Two micromechanical circumstances have been invoked to explain the remarkably high strength

data reported for the present materials: (i) the *t*- to *m*-ZrO_2 transformation and, (ii) the local residual microstresses arising from the thermal mismatch between the constituent phases. Since the Griffith's criterion of proportionality between fracture toughness and strength fails in explaining the experimental data collected in this composites, a critical stress criterion for microcracking failure, which arises from the phase transformation of the ZrO_2 matrix, has been adopted. This criterion explains acceptably the strength data of monolithic ZrO_2, in agreement with published values. To overlap the effect of phase transformation, local components of residual microstress are considered which may shield the microcracks triggering fracture above the critical stress level for transformation of the ZrO_2 matrix. Despite the simplistic notion of a nucleated microcracks shielded by residual microstresses, the present model enables one to explain the maximum strength experimentally found in the present composites in the range $0{\cdot}2 < V_f < 0{\cdot}4$.

Acknowledgements

The authors thank Dr G. Katagiri for his advice during the piezo-spectroscopy measurements and Miss M. Yoshioka for her help in the experimental work. This work has been supported by the Toray Foundation.

References

1. Swain, M. V., Inelastic deformation of Mg-PSZ and its significance for strength/toughness relationship of zirconia toughened ceramics. *Acta Metall.*, 1985, **33**, 2083–2088.
2. Hannink, R. H. J. and Swain, M. V., Magnesia partially stabilized zirconia: the influence of heat treatment on the thermomechanical properties. *J. Aust. Ceram. Soc.*, 1982, **18**, 53–62.
3. Budiansky, B., Hutchinson, J. W. and Lambropoulos, J. W., Continuum theory of dilatant transformation toughening in ceramics. *Int. J. Solids Struct.*, 1983, **19**, 337–355.
4. Rose, L. R. F. and Swain, M. V., Two R-curves for partially stabilized zirconia. *J. Am. Ceram. Soc.*, 1986, **69**, 203–207.
5. Tsukuma, K. and Shimada, M., Strength, fracture toughness and Vickers hardness of CeO_2-stabilized tetragonal ZrO_2 polycrystas (Ce-TZP). *J. Mater. Sci.*, 1985, **20**, 1178–1084.
6. Swain, M. V. and Rose, L. R. F., Strength limitations of transformation-toughened zirconia alloys. *J. Am. Ceram. Soc.*, 1986, **69**, 511–518.
7. Shikata, R., Urata, Y., Shiono, T. and Nishikawa, T., Strengthening of Y-PSZ-Al_2O_3 composite ceramics. *Jpn. J. Powder and Powder Metall.*, 1990, **37**, 357–361.
8. Shikata, R., Urata, Y., Shiono, T. and Nishikawa, T., Mechanical properties and characterization of $ZrO_2Al_2O_3$, composites with high fracture strength. *Jpn. J. Powder and Powder Metall* (in Japanese)., 1991, **38**, 369–373.
9. Shikata, R., Urata, Y., Shiono, T. and Nishikawa, T. Characterization and crack propagation behavior of ZrO_2-Al_2O_3 with high fracture strength. In *Transactions of the Materials Research Society of Japan*, Vol. 6, ed. S. Somiya, M. Doyama, M. Hasegawa and Y. Agata. Materials Research Society of Japan, Tokyo, 1992 pp. 50–65.
10. Forman, R. A., Piermarini, G. J., Barnett, J. D. and Block, S., Pressure measurements made by the utilization of ruby sharp line luminescence. *Science*, 1972, **176**, 284–285.
11. Ma, Q., Pompe, W., French, J. D. and Clarke, D. R., Residual stresses in Al_2O_3–ZrO_2 composites: a test of stochastic stress models. *Acta Metall. Mater.*, 1994, **42**, 1673–1681.
12. He, J. and Clarke, D. R., Determination of the piezospectroscopic coefficients for chromium-doped sapphire. *J. Am. Ceram. Soc.*, 1995, **78**, 1347–1353.
13. Nose, T. and Fujii, T., Evaluation of fracture toughness for ceramic materials by a single-edge-precracked-beam method. *J. Am. Ceram. Soc.*, 1988, **73**, 328–333..
14. Kreher, W. and Pompe, W., *Internal Stresses in Heterogeneous Solids*, Akademie-Verlag, Berlin, Germany, 1989.
15. Sergo, V., Wang, X.-I., Clarke, D. R. and Becher, P. F., Residual stresses in alumina/ceria-stabilized zirconia composites. *J. Am. Ceram. Soc.*, 1995, **78**, 2213–2214.
16. Sergo, V., Pezzotti, G., Yoshioka, M., Sbaizero, O. and Nishida, T., Grain size influence on residual stresses in alumina/zirconia composites. *Acta Mater.*, in press.
17. Irwin, G. R., Analysis of stresses and strains near the end of a crack traversing a plate. *J. Appl. Mech.*, 1957, **24**, 361–367.
18. Evans, A. G. and Cannon, R. M., Toughening of ceramics by martensitic transformation. *Acta Metall.*, 1986, **34**, 761–800.
19. Swain, M. V. and Hannink, R. H. J., R-curve behavior of zirconia ceramics. In *Advance in Ceramics, Vol. 12, Science and Technology of Zirconia II*, ed. N. Claussen *et al.* The American Ceramic Society, Columbus, OH, 1984.
20. Gong, S.-X. and Horii, H., General solution to the problem of microcracks near the tip of a main crack. *J. Mech. Phys. Solids*, 1989, **37**, 27–46.
21. Levin, I., Kaplan, W. D., Brandon, D. G. and Layyous, A. A., Effect of SiC submicrometer particle size and content on fracture toughness of alumina-SiC nanocomposites. *J. Am. Ceram. Soc.*, 1995, **78**, 254–256.
22. Sih, G. C., *Handbook of Stress Intensity Factors*. Lehigh University Press, Pennsylvania, 1973.
23. Sakai, M., Analysis of fiber bridging by extended Dugdale model. *Iron and Steel Inst. Jpn. Int.*, 1992, **32**, 937–942.
24. Selsing, J., Internal stresses in ceramics. *J. Am. Ceram. Soc.*, 1961, **44**, 419–421.
25. Kocks, U. F., A statistical theory of flow stress and workhardening. *Philos. Mag.*, 1996, **13**, 541–547.
26. Pezzotti, G., Lee, B.-T., Hiraga, K. and Nishida, T., A quantitative evaluation of microstructure in Si_3N_4/SiC platelet and particulate composites. *J. Mater. Sci.*, 1993, **28**, 4787–4798.
27. Pezzotti, G., Nishida, T. and Sakai, M., Physical limitation of the inherent toughness and strength in ceramic-ceramic and ceramic-metal nanocomposites. *J. Ceram. Soc. Jpn*, 1995, **103**, 9019–909.
28. Irwin, G. R., Fracture. In *Handbuch der Physik*, B.VI, ed. S. Flugge, Springer, Berlin, 1958, pp. 551–950.